Journal of Physics: Conference Series

PAPER • OPEN ACCESS

H infinity controller design to a rigid-flexible satellite with two vibration modes

To cite this article: A G de Souza and L C G de Souza 2015 *J. Phys.: Conf. Ser.* **641** 012030

View the article online for updates and enhancements.

You may also like

- Design of a new adaptive fuzzy controller and its application to vibration control of a vehicle seat installed with an MR damper
Do Xuan Phu, Do Kyun Shin and Seung-Bok Choi
- Profitability estimation of XYZ company using H-infinity and Ensemble Kalman Filter
M Y Anshori, T Herlambang, P Katias et al.
- NDM-based H-infinity robust control of parallel-connected grid-connected converters for V2G
Shilian Zhou, Longfang Li, Shujun Ben et al.



This content was downloaded from IP address 95.14.120.62 on 13/09/2023 at 13:14

Journal of Physics: Conference Series **641** (2015) 012030 doi:10.1088/1742-6596/641/1/012030

H infinity controller design to a rigid-flexible satellite with two vibration modes

A G de Souza[1], L C G de Souza[2]

[1] National Institute for Space Research (INPE), Av. dos Astronautas 1758, 12227-010 Sao Jose dos Campos, SP, Brazil.
[2] Brasilia University, Campus Gama, Area Especial de Industria-A-UnB, 72444-240 Brasilia, DF, Brazil.

E-mail: alain.souza@inpe.br

Abstract. The satellite attitude control system (ACS) design becomes more complex when the satellite structure has components like, flexible solar panels, antennas and mechanical manipulators. These flexible structures can interact with the satellite rigid parts during translational and/or rotational manoeuvre damaging the ACS pointing accuracy. Although, a well-designed controller can suppress such disturbances quickly, the controller error pointing may be limited by the minimum time necessary to suppress such disturbances thus affecting the satellite attitude acquisition. This paper deals with the rigid-flexible satellite ACS design using the H infinity method. The rigid-flexible satellite is represented by a beam connected to a central rigid hub at one end and free at the other one. The equations of motions are obtained considering small flexible deformations and the Euler-Bernoulli hypothesis. The results of the simulations have shown that the H-infinity controller was able to control the rigid motion and suppress the vibrations.

1. Introduction

There are several methodologies [1] to design satellite ACS, depending on the control system complexity; computer simulation cannot be the more appropriate one. Experimental platforms [2] have the important advantage of allowing the satellite dynamics representation in laboratory to accomplish experiments and simulations to evaluate satellites ACS. Experimental test has also the possibility of introducing more realism than the simulation; but it has the difficulty of reproducing zero gravity and torque free space condition. Examples of simulator dynamics and control system experimental investigations can be found in [3, 4]. A classic case of a phenomenon that was not investigated experimentally before launch, was the dissipation energy effect that has altered the satellite Explorer I rotation [5]. Several institutions and universities [6, 7] are investigating and testing the ACS performance by experimental prototypes. In [8,9] it was showed that the influence of the non-linearities introduced by the slosh motion, the panels flexibility and the system parameters variation can degrade the control system performance, indicating the necessity of new robust control technique. Examples of multi-objectives methods to design controllers space system can be found in [10, 11]. In this paper one investigates the rigid-flexible satellite ACS design using the H infinity method [12, 13]. The rigid-flexible satellite model is represented by the Rotary flexible link module which consists of a rigid central hub


Content from this work may be used under the terms of the Creative Commons Attribution 3.0 licence. Any further distribution of this work must maintain attribution to the author(s) and the title of the work, journal citation and DOI.
Published under licence by IOP Publishing Ltd

connected to a flexible appendage [14]. The model used can be interpreted as a solar panel or a flexible antenna coupled to a rigid satellite.

2. Rigid-flexible Satellite Model

The figure 1 shows the representations of the rigid-flexible satellite model; which consist of a rigid central part and by a flexible beam with the mass in the end. The actuator is located in the central part, and it is responsible for the control of the horizontal planar movement of the rigid structure and by the elastic displacement, where (X_0, Y_0) and (X, Y) are the coordinates system before and after deformation, respectively. The rigid central hub has radius R, the actuator rotor has viscous friction bm, and inertia J_{rotor} and develops a torque $\tau(t)$; the flexible beam has uniform linear mass density ρ, uniform bending stiffness EI and length L; the flexible beam deformation is $w(x,t)$; and the tip mass is m_{tip} and inertia J_{tip}; $\alpha(t)$ represent the tip angle and $\theta(t)$ is the rigid angle displacement; and $s(x)$ represent the distance between the referential axis to an element of mass in the link.

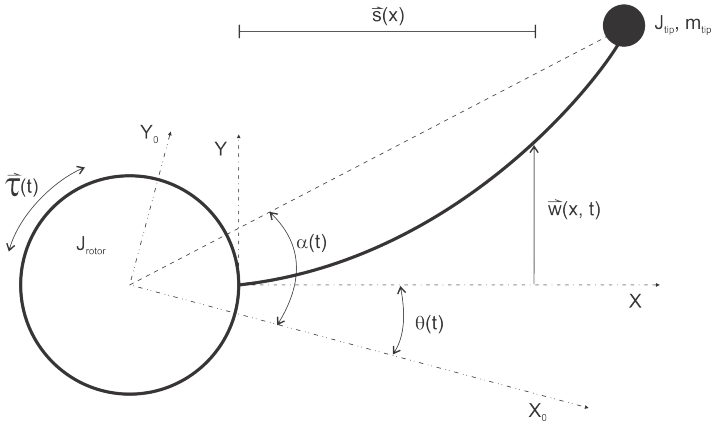


Figure 1. Rigid-flexible satellite parameters

The equations of motion of the entire structure are derived using the Lagragian approach [5] combined with the assumed modes method. The flexible link is modeled as an Euler-Bernoulli beam. The free vibration of the link is described by the partial differential equation

$$EI\frac{\partial^4 w(x,\,t)}{\partial x^4} + \rho\frac{\partial^2 w(x,\,t)}{\partial t^2} = 0 \tag{1}$$

with boundary condition:

$$w(0,\,t) = 0;\;\; \frac{\partial w(0,\,t)}{\partial x} = 0;\;\; \frac{\partial^2 w\,(L,\,t)}{\partial x^2} = 0; \qquad \frac{m_{tip}}{EI}\frac{\partial^2 w(L,t)}{\partial t^2} = \frac{\partial^3 w(L,t)}{\partial x^3} \tag{2}$$

Solving this partial differential equation (PDE) of motion one obtains:

$$Y\,(x) = C_1\left(\cosh\left(\beta_i x\right) - \cos\left(\beta_i x\right) - \left(\frac{\left(\cosh\left(\beta_i L\right) + \cos\left(\beta_i L\right)\right)}{\left(senh\left(\beta_i L\right) + sen\left(\beta_i L\right)\right)}\right)\left(senh\left(\beta_i x\right) - sen\left(\beta_i x\right)\right)\right) \tag{3}$$

where: $\omega_i^2/C_2 = \beta_i^2$; $\omega_i^2 = C^2\beta_i^4$; $\omega_i = \beta_i^2\sqrt{(EI/\rho)}$; and C_1 is a normalization constrain and β_i is the real positive squares of the transcendental equation:

$$\cos\left(\beta_i L\right)\cosh\left(\beta_i L\right) - K\left(\cos\left(\beta_i L\right)\sinh\left(\beta_i L\right) - \cosh\left(\beta_i L\right)\sin\left(\beta_i L\right)\right) = 1 \tag{4}$$

with, $K = m_{tip}/\rho$.

The total kinetic energy [7] is given by the sum of the kinetic energies of the rotor, tip mass and a mass element in the link ($T = T_{rotor} + T_{dm} + T_{tip}$), which is given by

$$\begin{array}{c} T = \frac{1}{2}\dot{\theta}^2\left[J_{rotor} + \rho\left[\int_0^L w^2 dx + \frac{1}{3}(R+L)^3 - \frac{1}{3}R^3\right] + m_{tip}\left[w_L^2 + (R+L)^2\right] + J_{tip}\right] + \\ + \frac{1}{2}\dot{\theta}\left[2\rho\int_0^L \dot{w}(R+s)dx + 2m_{tip}\dot{w}_L + J_{tip}\left(\frac{\partial \dot{w}}{\partial x}\right)\right] + \frac{1}{2}\left[\rho\int_0^L \dot{w}^2 dx + m_{tip}\left(\frac{\partial \dot{w}}{\partial x}\right)\right] \end{array} \tag{5}$$

and the potential energy is

$$V = \frac{1}{2}EI\int_o^L \left(\frac{\partial^2 w}{\partial x^2}\right)^2 dx \tag{6}$$

One admits that the dissipation energy caused by the viscous damping of the rotor and by the deformation of the beam is given by

$$R = \frac{1}{2}b_m\dot{\theta}^2 + \frac{1}{2}K_e EI\int_0^L \left(\frac{\partial^2 \dot{w}}{\partial x^2}\right)^2 dx \tag{7}$$

According with the assumed mode method, one can write the elastic deflection as a function of the modal form ($\varphi_i(x)$) and a generalized coordinates of the deflection ($\eta_i(t)$).

$$w(x,\,t) = \sum_{i=1}^{n} \varphi_i(x)\,\eta_i(t) \tag{8}$$

The form function normalization rules are given by

$$\rho\int_o^L \varphi_i(x)\,\varphi_j(x)\,dx + m_{tip}\varphi_i(L)\,\varphi_j(L) = 0 \quad i \neq j; \qquad \rho\int_o^L \varphi_i^2(x)\,dx + m_{tip}\varphi_i^2 = 1 \quad i = j \tag{9}$$

As a result, the solution of the PDE [7] for the modal forms is:

$$\varphi_i(x) = C_1\left(\cosh(\beta_i x) - \cos(\beta_i x) - \left(\frac{(\cosh(\beta_i L) + \cos(\beta_i L))}{(senh(\beta_i L) + sen(\beta_i L))}\right)(senh(\beta_i x) - sen(\beta_i x))\right) \tag{10}$$

where the constant C_1 is defined by the normalizations rules. The angular frequency is $\omega_i = \beta_i^2\sqrt{(EI/\rho)}$.

For this paper one assumes two modes of vibration, where rigid angular displacement (θ) and the deflection variables (η_i) are used as generalized coordinates in the derivation of the equation of motion. For convenience one uses the matrix form, and then the vectors η_i and ϕ_i are represented by the matrices q and ϕ.

Using the eq. (5) e eq. (6) one obtains the Lagragian

$$\begin{array}{c} \mathcal{L} = \frac{1}{2}\dot{\theta}^2\left[J_{rotor} + q^T\rho\int_0^L \phi\phi^T dx q + \rho\frac{1}{3}(R+L)^3 + m_{tip}\left(q^T\phi_L\phi_L^T q + (R+L)\right)^2 + J_{tip}\right] + \\ + \frac{1}{2}\dot{\theta}\left[2\rho\dot{q}^T\int_0^L \phi\,(R+s)\,dx + 2m_{tip}\dot{q}^T\phi_L\,(R+L) + J_{tip}\dot{q}^T\phi'\right] + \\ + \frac{1}{2}\left[\rho\dot{q}^T\int_0^L \phi\phi^T dx\dot{q} + m_{tip}\dot{q}^T\left(\phi_L\phi_L^T\right)\dot{q} + J_{tip}\dot{q}\left(\phi'\phi^{T'}\right)\dot{q}\right] - \frac{1}{2}q^T EI\int_0^L \phi''\phi^{T''} dx q \end{array} \tag{11}$$

Applying the Lagragian methodology [7], the Lagrange equation is

$$\frac{d}{dt}\left[\frac{\partial}{\partial p_i}\mathcal{L}\right] - \frac{\partial}{\partial p_i}\mathcal{L} + \frac{\partial}{\partial p_i}R = Q_i \tag{12}$$

where $p_i = \{\theta,\ q\}$ e $Q = \{\tau, 0\}$, with that one have the following nonlinear dynamic, represented by a matrix form, is obtained.

$$\begin{bmatrix} I_t + q^T C_{rr} q & M_{rf}^T \\ M_{rf} & M_{ff} \end{bmatrix} \begin{bmatrix} \ddot{\theta} \\ \ddot{q} \end{bmatrix} + \begin{bmatrix} b_m & 0 \\ 0 & B_{ff} \end{bmatrix} \begin{bmatrix} \dot{\theta} \\ \dot{q} \end{bmatrix} + \begin{bmatrix} 0 & 0 \\ 0 & K_{ff} \end{bmatrix} \begin{bmatrix} \theta \\ q \end{bmatrix} + \begin{bmatrix} \dot{\theta} q^T C_{rr} \dot{q} \\ -\dot{\theta}^2 C_{rr} q \end{bmatrix} = \begin{bmatrix} \tau \\ 0 \end{bmatrix} \tag{13}$$

where,

$$\begin{array}{l} \eta_i = \mathbf{q};\quad \varphi(x,\,t) = \phi;\quad \varphi(L,\,t) = \phi_L;\quad \mathbf{K}_{ff} = EI\int_0^L \phi''\phi''^T dx;\quad \mathbf{B}_{ff} = K_e EI\int_0^L \phi''\phi''^T dx \\ \mathbf{C}_{rr} = \rho\int_0^L \phi\phi^T dx + m_{tip}\phi_L{\phi_L}^T;\quad \mathbf{M}_{ff} = \rho\int_0^L \phi\phi^T dx + m_{tip}\phi_L\phi_L^T + \frac{1}{2}J_{tip}{\phi_L}'{\phi_L}'; \end{array} \tag{14}$$

To obtain a linear model the nonlinear terms $q^T C_{rr} q$, $q^T C_{rr} q$ e $-\dot{\theta}^2 C_{rr} q$ are neglected due to the fact that they are relatively very small [4]. So writing eq.(

$$\begin{bmatrix} \dot{X}_1 \\ \dot{X}_2 \end{bmatrix} = \begin{bmatrix} 0 & I \\ -M^{-1}K & -M^{-1}D \end{bmatrix} \begin{bmatrix} X_1 \\ X_2 \end{bmatrix} + \begin{bmatrix} 0 \\ M^{-1}Q \end{bmatrix} u \tag{15}$$

with $X = \begin{bmatrix} \theta & \eta_1 & \eta_2 & \dot{\theta} & \dot{\eta}_1 & \dot{\eta}_2 \end{bmatrix}$ is the states vectors and the control $u = K_{H_\infty} X$, where K_{H_∞} is the gain calculate by the H infinity method [15].

3. H infinity control method

One great advantage of the H_∞ control method is the possibility of designing robust controllers with respect to structured uncertainty at the same time that is possible to obtain good performance with respect to unstructured uncertainty. As a result, the H_∞ controller design is a multi-objective control problem where performance improvement and good robustness requirement are functions of the weighting functions selection as it will be explained in the sequel [15].

The norm H_∞ of the system transfer function $G(s)$ can be expressed by the major value of the singular value (σ) in frequency domain given by:

$$\|G(s)\|_\infty = \max_\omega \bar{\sigma}\left(G(j\omega)\right) \tag{16}$$

The H_∞ norm is usually computed numerically from a state-space realization as the smallest value of γ such that the Hamiltonian matrix eq. (17) has no eigenvalues on the imaginary axis [6],

$$\mathrm{H} = \begin{bmatrix} A + BR^{-1}D^T C & BR^{-1}B^T \\ -C^T\left(I + DR^{-1}D^T\right)C & -\left(A + BR^{-1}D^T C\right)^T \end{bmatrix} \tag{17}$$

where A, B, C e D are the space state matrices and $R = \gamma^2 I - D^T D$. This is an interactive procedure; where one may start with a large value of γ and reduce it until imaginary eigenvalues for H appear. Basically the H infinity control method consists of calculating a gain K that minimizing the H_∞ norm of the transfer function of the closed loop [15].

The closed loop transfer function is given by:

$$\begin{bmatrix} z \\ v \end{bmatrix} = P(s) \begin{bmatrix} \omega \\ u \end{bmatrix} = \begin{bmatrix} P_{11}(s) & P_{12}(s) \\ P_{21}(s) & P_{22}(s) \end{bmatrix} \begin{bmatrix} \omega \\ u \end{bmatrix} \tag{18}$$

where, $u = K(s)v$. In the other hand one can write as:

$$F_l(P,K)\,\omega = P_{11} + P_{12}K(I - P_{22}K)^{-1}P_{21} \tag{19}$$

Minimizing the H norm:

$$\|F_l(P,K)\|_\infty = \max_\omega \bar{\sigma}\left(F_l(P,K)(j\omega)\right) \quad \|F_l(P,K)\|_\infty < \gamma \tag{20}$$

3.1. A weighting functions

The selection of weighting functions for a specific design problem often involves many interactions and fine-tuning. It is hard to give a general formula for the weighting functions that will work in every case [15]. Therefore in the literatures [16] is possible to find some suggestions, and/or starting point for analysis and iterations to find a starter weighting function. Then like was suggesting by [15] one uses the follow functions:

$$W_S = \left(\frac{\frac{s}{\sqrt[k]{M}} + \omega_b}{s + \sqrt[k]{A}\omega_b}\right)^k, \; W_T = \left(\frac{s + \frac{\omega_{bc}}{\sqrt[k]{M}}}{\sqrt[k]{A}s + \omega_{bc}}\right)^k, \; W_{KS} = cte \tag{21}$$

For the study case, the constants are: k- adjust the roll off ($k = 1$); ω_b- equal the value of the bandwidth of the plant ($_b = 0,03rad/s$; as showed in the figure 2); ω_{bf} - proportional to ($\omega_{bf} = 100 \cdot \omega_b$); A - limited the steady-error ($A = 10^{-3}$);M - limited the Overshoot ($M = 10$).

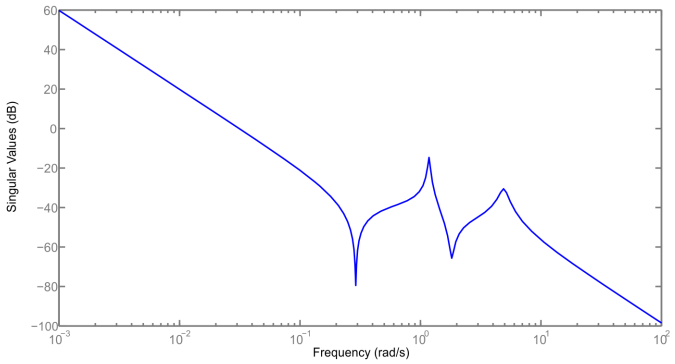


Figure 2. Singular values of the plant.

4. Results of the simulations

For the simulation the constant parameter are: $R = 0.05m$, $bm = 0.15m^2/s$, $J_{rotor} = 0.3kgm^2$, $L = 1m$, $\rho = 2700kg/m$, $ke = 0.03$, $EI = 18.4Nm^2$, $m_{tip} = 0.25kg$ and $J_{tip} = 0.04kgm^2$. The objective of the control is stabilize the tip mass angle (α) of the flexible link in a neutral position ($0°$). The angle α given by:

Appling the H infinity control method in the plant model showed in the eq. (15), one obtains the fallow results for the initial response (the link is in the position). In the figure 3 are presented the results the simulation for the states: the rigid angular displacement, the first vibration mode and second vibration mode, and its variation with respect the time, respectively. Figure 3 shows that the H_∞ control law stabilizes rigid angular displacement (θ) around in 60 seconds, the first

vibration mode (η_1) stabilizes around 80 seconds and the second vibration mode (η_2) stabilizes around 60 seconds. Figure 4 shows that the H_∞ control law stabilizes the derivate of the states ($d\theta/dt$) and ($d\eta_1/dt$) around in 80 seconds, while ($d\eta_2/dt$) stabilizes around 40 seconds.

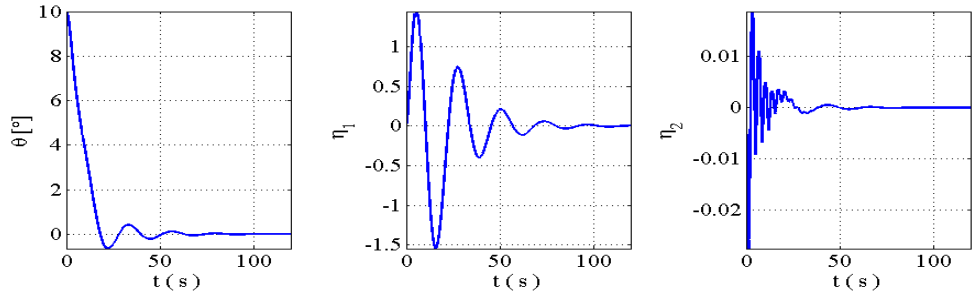


Figure 3. H_∞ control of the attitude and flexibility.

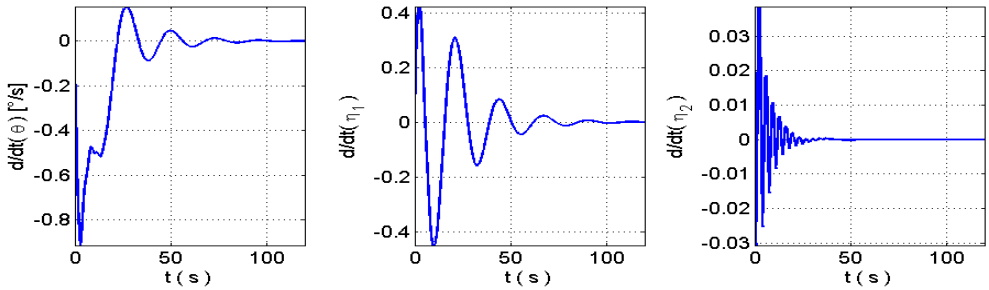


Figure 4. H_∞ control of the attitude and flexibility rates

Figure 5 shows the behavior of the tip mass angle (α) ; starting in an initial position 10° and finishing in a position 0°. The H_∞ control performance concludes in 100 seconds. Figure 6 shows the H_∞ control effort (the torque generate by the rotor) has the maximum about $3.8Nm$ and $-4.0Nm$.

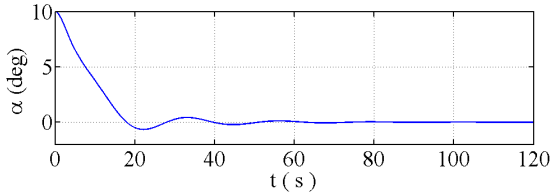


Figure 5. H_∞ control of the tip-mass.

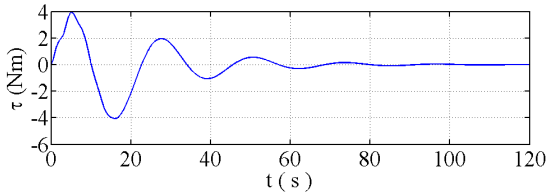


Figure 6. H_∞ control effort.

5. Conclusion

In this paper one applies the H-infinity method to design the attitude control system (ACS) for a rigid-flexible satellite. The satellite model is represented by a flexible beam connected to a rigid central hub with a tip mass in its free end. The Lagrange approach is used to obtain equations of motions considering small flexible deformations. The simulations results have showed that the H-infinity controller was able to control the rigid motion and suppress the vibrations. That good controller performance was obtained by selection of weighting functions parameters for that specific problem. The results has also showed that the model is representative of rigid-flexible

satellite with one panel and that H_∞ controller has achieves the objectives controlling the rigid angular displacement and suppressing the vibrations modes, bringing the tip mass angle to a neutral position with acceptable control effort in a short time interval. Finally, one observes that the H_∞ control performance is dependent of weighting functions, so better performance can be archived if more investigation is spend in the selection of the weighting functions.

References

[1] Hall, C.D. , Tsiotras and Shen, H. Tracking Rigid Body Motion Using Thrusters and Momentum Wheels, *Journal of the Astronautical Sciences*, 2002.
[2] Schwartz, J. L.; Peck, M. A. and Hall, C. D. Historical review of air-bearing spacecraft simulators. *Journal of Guidance, Control and Dynamics*, 26, 4, (2003),513-522.
[3] Conti G.T. and Souza, L.C.G. Satellite attitude control system simulator. *Journal of Shock and Vibration*. 15, 3-4, (2008), 395-402.
[4] Souza, L.C.G. ; Gonzles,R.G.Application of the State-dependent Riccati Equation and Kalman Filter Techniques to Design of a Satellite Control System. *Shock and Vibration*, v. 19, p. 22-28, 2012.
[5] Kaplan M. H, *Modern Spacecraft Dynamics and Control*, John Wiley Sons, NY, 1976.
[6] Tsiotras, P. A Spacecraft Simulator for Research and Education, Georgia Institute of Technology, EUA, 2007.
[7] Souza, A. G. ; Souza, L. C. G. Design of Satellite Attitude Control System Considering the Interaction between Fuel Slosh and Flexible Dynamics during the System Parameters Estimation. *Applied Mechanics and Materials*, v. 706, p. 14, 2015.
[8] Bigot, P., and Souza, L. C. (2014). Investigation of the State Dependent Riccati Equation (SDRE) adaptive control advantages for controlling non-linear systems as a flexible rotatory beam. *International journal of systems applications, engineering and development.*Vol.8,pp 92-99.
[9] Mainenti-Lopes, I ; Souza, L. C. G. ; Souza, F.L . Design of a nonlinear controller for a rigid-flexible satellite using multi-objective Generalized Extremal Optimization with real codification. *Shock and Vibration*, v. 19, p. 1-10, 2012.
[10] Pinheiro, E. R.; Souza, L. C. G.. Design of the Microsatellite Attitude Control System Using the Mixed Method via LMI Optimization. *Mathematical Problems in Engineering (Print)*, v. 2013, p. 1-8, 2013.
[11] Souza, L. C. G. ; Control of a Rigid-Flexible Satellite Solar Panel with Non-collocated Sensor/Actuator. Journal of Mechanics Engineering and Automation, v. 5, p. 173-179, 2015.
[12] Souza, L C G ; Souza, A. G. . Satellite Attitude Control System Design considering the Fuel Slosh Dynamics. *Shock and Vibration*, v. 2014, p. 1-8, 2014.
[13] Quanser homepage. at: http://www.quanser.com/.
[14] Skogestad, S.; Postlethwaite, I. *Multivariable Feedback Control Analysis and Design*. 2. ed. Chichester: John Wiley Sons, 2001
[15] Zhou, K. ; Doyle, J. C. *Essentials of Robust Control*. New Jersey: Prentice Hall, 1998.